Article

pubs.acs.org/Biomac

Hyperbranched Copolymers Based on Glycidol and Amino Glycidyl Ether: Highly Biocompatible Polyamines Sheathed in Polyglycerols

Suhee Song,[†,‡] Joonhee Lee,[†,‡] Songa Kweon,[‡] Jaeeun Song,[‡] Kyuseok Kim,[§] and Byeong-Su Kim*[,‡]

[‡]Department of Chemistry, School of Natural Science, Ulsan National Institute of Science and Technology (UNIST), Ulsan 44919, Korea

[§]Department of Emergency Medicine, Seoul National University Bundang Hospital, Seongnam, Gyeonggi-do 13620, Korea

Supporting Information

ABSTRACT: Functional hyperbranched polyglycerols (PGs) have recently garnered considerable interest due to their potential in biomedical applications. Here, we present a one-pot synthesis of hyperbranched PGs possessing amine functionality using a novel amino glycidyl ether monomer. A Boc-protected butanolamine glycidyl ether (BBAG) monomer was designed and polymerized with glycidol (G) through anionic ring-opening multibranching polymerization to yield a series of hyperbranched P(G-*co*-BBAG) with controlled molecular weights (4800−16700 g/mol) and relatively low molecular weight distributions (1.2−1.6). The copolymerization and subsequent deprotection chemistry allow the incorporation of an adjustable fraction of primary amine moieties (typically, 5−20% monomer ratio) within the hyperbranched PG backbones, thus providing potentials for varying charge densities and functionality in PGs. The copolymerization kinetics of G and BBAG was also evaluated using a quantitative in situ ^{13}C NMR spectroscopic analysis, which revealed gradient copolymerization between the comonomers. The free amine groups within the deprotected P(G-*co*-BAG) copolymer were further utilized for a facile conjugation chemistry with a model molecule in a quantitative manner. Furthermore, the superior biocompatibility of the prepared P(G-*co*-BAG) polymers was demonstrated via cell viability assays, outperforming many existing polyamines possessing relatively high cytotoxicity. Taken together, the biocompatibility with facile conjugation chemistry of free amine groups sheathed within the framework of hyperbranched PGs holds the prospect of advancing biological and biomedical applications.

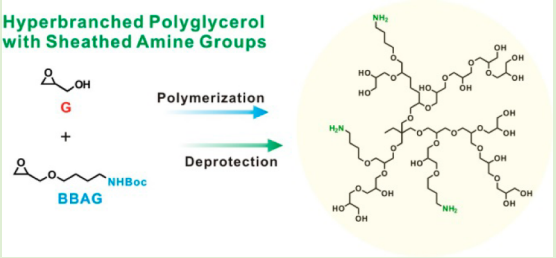

INTRODUCTION

Poly(ethylene glycol) (PEG) represents the most important class of polyethers with a broad range of potential impact in biological fields and pharmaceutical industry, owing to its superior biocompatibility and low immunogenicity and toxicity.[1−7] A fundamental challenge with PEG, however, lies in the lack of functionality within the polymer backbone, limiting the tunability for a wider range of applications.[7−9] As an alternative to linear polyether analogues of PEG, hyperbranched polyglycerols (PGs) have recently attracted significant attention due to their unique three-dimensional architecture that comprises a polyether backbone with a large number of functional hydroxyl groups together with their facile synthetic nature.[7,10−14]

Recent synthetic advancements have allowed the development of well-defined and complex architectures of PGs with a broad range of molecular weights and functionality, typically using a ring-opening multibranching polymerization of glycidol (G) and functional epoxide monomers.[10,15−18] To date, in order to build the complex architectures of PGs and tailor their physicochemical properties, many novel functional epoxide monomers have been developed.[7,10,19,20] In particular, polyethers with amine functional groups have been actively investigated because of their high potential in surface modification and biological conjugation.[21−25] As direct polymerization of an epoxide monomer bearing primary amine groups is not feasible, two approaches are typically employed to introduce amine groups on polyethers, such as postpolymerization functionalization and direct copolymerization using protected monomeric building blocks. Koyama et al. first introduced primary amine moieties via copolymerization of ethylene oxide with allyl glycidyl ether (AGE), followed by thiol−ene coupling of 2-aminoethanethiol to the AGE.[26] In another approach, Frey and co-workers have reported a series of protected glycidyl amine derivatives as novel functional monomers, including *N*,*N*-dibenzyl amino glycidol,[27] *N*,*N*-diallyl glycidyl amine,[28] and epicyanohydrin.[29] Recently, Satoh and co-workers reported the use of *N*,*N*-disubstituted glycidyl amine derivatives to obtain well-defined polyethers with various pendant amine groups as well.[30] In another notable effort, Lynd and Hawker's group reported the use of *N*,*N*-diisopropyl ethanolamine glycidyl ether to investigate the pH-responsive behavior of polyethers in physiologically relevant conditions.[31] Nonetheless, many of these studies were limited to the investigation of random copolymer systems in linear polyethers such as PEG.

In a continuation of our endeavor to develop functional hyperbranched PGs for biomedical applications,[32−34] we now report on the one-pot synthesis of a series of hyperbranched PGs possessing amino functionality by using a Boc-protected butanolamine glycidyl ether monomer (BBAG; Figure 1). Specifically, *t*-butyl 4-(oxiran-2-ylmethoxy)butylcarbamate (BBAG) was designed and polymerized through anionic ring-opening multibranching polymerization to yield a series of hyperbranched P(G-*co*-BBAG) with controlled molecular weights (4800−16700 g/mol) and relatively low molecular weight

Received: July 25, 2016
Revised: September 28, 2016
Published: October 14, 2016

DOI: 10.1021/acs.biomac.6b01136
Biomacromolecules 2016, 17, 3632−3639

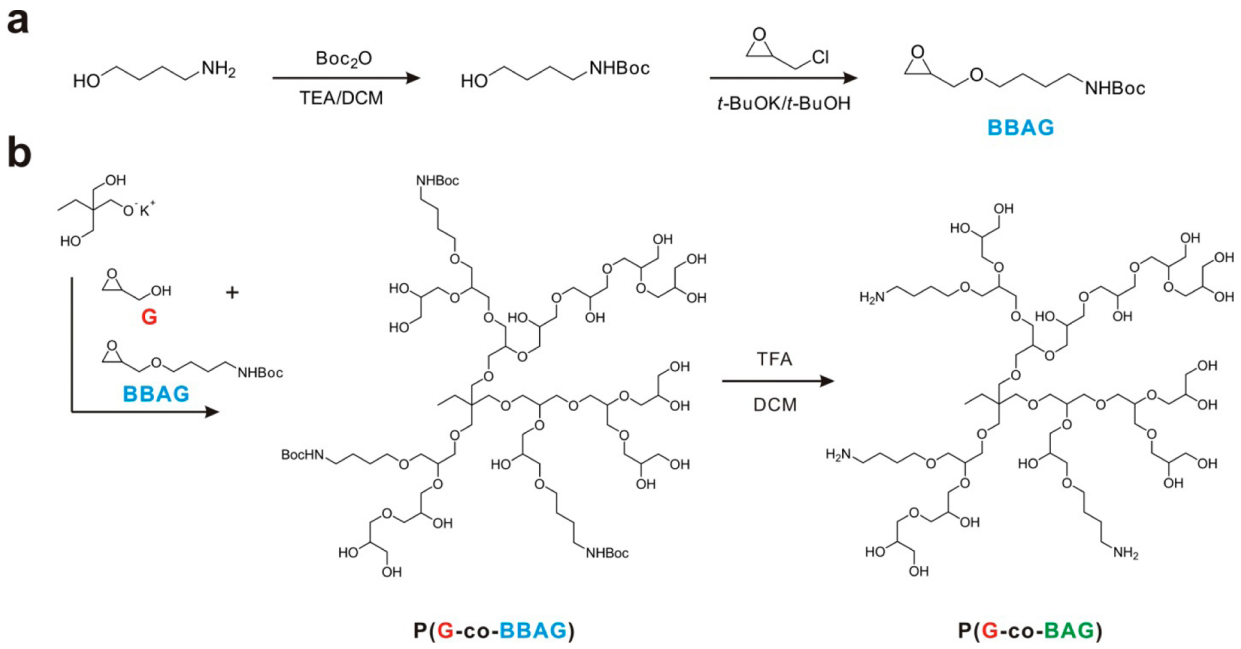

Figure 1. Synthetic pathways of (a) the BBAG monomer and (b) anionic ring-opening copolymerization of P(G-*co*-BBAG) and subsequent deprotection to yield P(G-*co*-BAG).

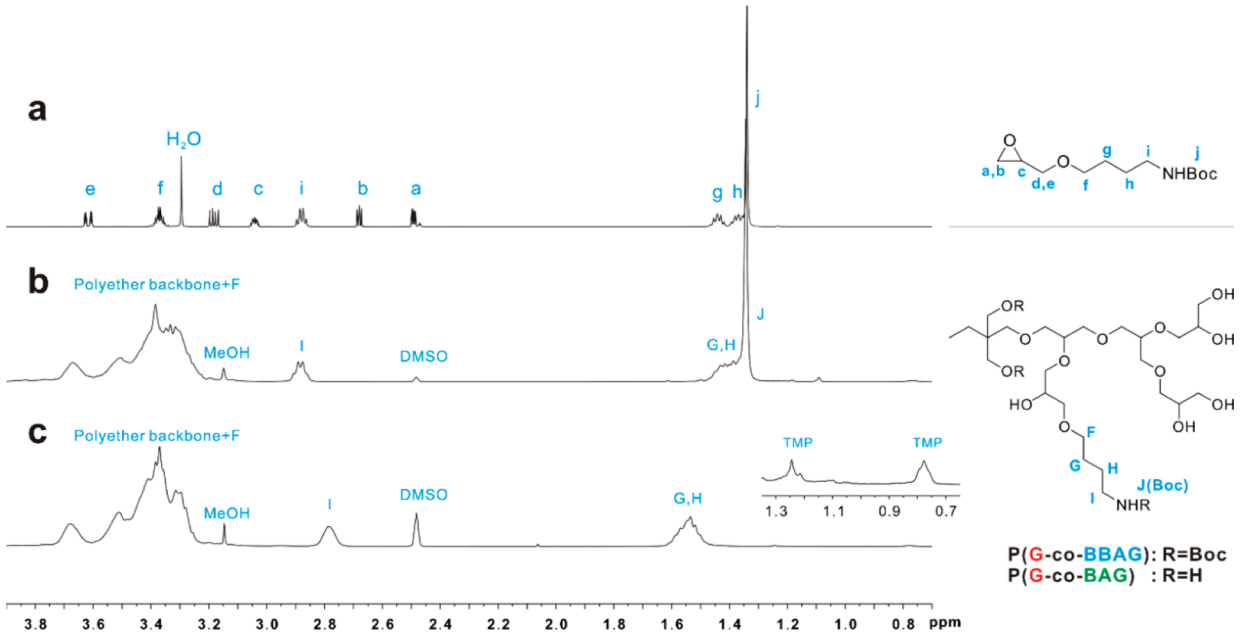

Figure 2. ^{1}H NMR spectra of (a) BBAG monomer, (b) P(G_{113}-*co*-$BBAG_{21}$) copolymer (polymer 7), and (c) deprotected P(G_{113}-*co*-BAG_{21}) copolymer measured in DMSO-d_6.

distributions (M_w/M_n = 1.2−1.6). The copolymerization and subsequent deprotection chemistry allowed for the incorporation of an adjustable fraction of primary amine moieties (typically, 5−20% monomer ratio) within the hyperbranched PG backbones, thus, providing the potential for varying charge densities and functionality within the hyperbranched PG. We also investigated the copolymerization kinetics of G and BBAG using a quantitative in situ ^{13}C NMR spectroscopic analysis. The free amine groups within the deprotected P(G-*co*-BAG) copolymers were further utilized for facile conjugation chemistry with a model molecule in a quantitative manner. Furthermore, we demonstrated the superior biocompatibility of the prepared polymers via cell viability assays.

EXPERIMENTAL SECTION

Materials. All reagents and solvents were purchased from Sigma-Aldrich and Acros and used as received unless otherwise stated. All deuterated NMR solvents such as $CDCl_3$, D_2O, and DMSO-d_6 were purchased from Cambridge Isotope Laboratory.

Characterization. ^{1}H and ^{13}C NMR spectra were acquired using a 400-MR DD2 (400 MHz) and VNMRS 600 (600 MHz) spectrometer using $CDCl_3$, D_2O, and DMSO-d_6 as solvents and chemical shifts were recorded in ppm units with TMS as an internal standard. The number-(M_n) and weight-averaged (M_w) molecular weights and molecular-weight distribution (M_w/M_n) were measured using gel permeation chromatography (GPC, Agilent Technologies 1200 series) with a polystyrene (PS) standard and 0.010 M lithium bromide containing

DOI: 10.1021/acs.biomac.6b01136
Biomacromolecules 2016, 17, 3632−3639

dimethylformamide (DMF) as an eluent at 30 °C with a flow rate of 1.00 mL/min. Matrix-assisted laser desorption and ionization time-of-flight (MALDI-ToF) mass spectrometry measurements were carried out on an Ultraflex III MALDI mass spectrometer with α-cyano-4-hydroxycinnamic acid as the matrix. Differential scanning calorimetry (DSC) was performed using a differential scanning calorimeter (Q200 model, TA Instruments) in the temperature range of −80−50 °C at a heating rate of 10 K/min under nitrogen. The zeta potential was measured using a Malvern Zetasizer Nano-ZS.

Protection of 4-Amino-1-butanol. The precursor, *t*-butyl *N*-(4-hydroxybutyl)carbamate was synthesized according to the literature procedure with slight modification.[35] To a solution of 4-amino-1-butanol (10 g, 112 mmol) and triethylamine (17.1 mL, 123 mmol) in dichloromethane (CH_2Cl_2, 35 mL), a solution of di-*tert*-butyl-dicarbonate (25.7 g, 118 mmol) in CH_2Cl_2 (100 mL) was added dropwise over 30 min at room temperature. The mixture was stirred at room temperature for 6 h and the reaction mixture was concentrated under reduced pressure. The crude mixture was dissolved in CH_2Cl_2 and washed with water and then with brine. The organic phase was dried over Na_2SO_4 and concentrated under reduced pressure. The residue was purified by flash column chromatography eluting with 10% methanol in CH_2Cl_2 to give a compound as colorless oil.

Synthesis of BBAG Monomer. A solution of *t*-butyl *N*-(4-hydroxybutyl)carbamate (14.5 g, 76.6 mmol) in *t*-butanol (100 mL) was slowly added to a solution of potassium *t*-butoxide (8.50 g, 76.6 mmol) in *t*-butanol (100 mL) with stirring for 15 min at room temperature under argon. After stirring for an additional 15 min, excess epichlorohydrin (35.9 mL, 459 mmol) was added dropwise for 30 min. The solution was stirred at room temperature for 24 h after which additional water (100 mL) and CH_2Cl_2 (200 mL) were added. The aqueous phase was extracted with CH_2Cl_2 and combined organic layers were dried over $MgSO_4$. The organic phase was concentrated under reduced pressure and the residue was purified by flash column chromatography with CH_2Cl_2/hexane (1:100 v/v) eluent to give 11.2 g (60%) of the BBAG monomer as a colorless oil. The synthesis of the BBAG monomer was successfully confirmed through various characterizations, including ^{1}H and ^{13}C NMR, COSY, HMQC, and DEPT spectroscopy and ESI-MS (see Figure 2 for corresponding peak assignments and Figures S1−S4 in the Supporting Information). ^{1}H NMR (600 MHz, DMSO-d_6): δ ppm 3.61 (dd, 1H, J = 11.6 and 2.8 Hz, e), 3.34−3.40 (m, 2H, f), 3.18 (dd, 1H, J = 11.5 and 6.3 Hz, d), 3.03−3.05 (m, 1H, c), 2.88 (q, 2H, J = 6.7 Hz, i), 2.68 (dd, 1H, J = 4.3 and 5.1 Hz, b), 2.49 (dd, 1H, J = 5.1 and 2.6 Hz, a), 1.42−1.47 (m, 2H, g), 1.36−1.39 (m, 2H, h), 1.34 (s, 9H, j). ^{13}C NMR (150 MHz, DMSO-d_6): δ ppm 158.66, 80.38, 74.24, 73.29, 53.41, 46.46, 42.88, 31.34, 29.65, 29.34. MS (m/z + Na^+, ESI^+) Calcd for $C_{12}H_{23}NO_2$, 268.3; found, 268.3

Synthesis of P(G_{56}-*co*-$BBAG_2$) (Polymer 1). Trimethylolpropane (TMP; 54.6 mg, 0.407 mmol) was placed in a two-neck round-bottom flask. Potassium methoxide in methanol (25 wt %, 45 μL, 0.163 mmol) was diluted with 0.70 mL of methanol and then added to the flask and stirred for 30 min at room temperature under an argon atmosphere. Excess methanol was removed using a rotary evaporator and the resulting product was dried in a vacuum oven at 90 °C for 3 h to yield a white salt of the initiator. The flask was then purged with argon and heated to 90 °C. A mixture of *t*-butyl 4-(oxiran-2-ylmethoxy)-butylcarbamate (BBAG; 0.30 g, 1.22 mmol) and glycidol (G; 1.54 g, 23.23 mmol) was added dropwise over 12 h using a syringe pump. After complete addition of the monomer, the reaction was continued for an additional 5 h. The resulting P(G_{56}-*co*-$BBAG_2$) copolymer was dissolved in 1.0 mL of methanol; the homogeneous polymer solution was then precipitated in excess diethyl ether, and the precipitate was washed twice using diethyl ether. The resulting polymer was dried under vacuum at 90 °C for 1 day. All polymers synthesized in this study were isolated in approximately 90% yield. The M_n of the P(G_{56}-*co*-$BBAG_2$) polymer was determined to be 4773 g/mol, as calculated from the NMR data (see Figure S5 in the Supporting Information) using the following equation: number of repeating units (BBAG) = 17.25 (integration value)/9 (number of protons of *t*-butyl of BBAG) = 2, number of repeating units (G) = [292.13 (integration value) − {(2 (number of BBAG repeating units) × 7 (number of protons of BBAG except *t*-butyl)}]/5 (number of protons of the G monomer (5H)) = 56; M_n = 74.08 (molecular weight of the G monomer) × 56 + 245.32 (molecular weight of the BBAG monomer) × 2 + 134.17 (molecular weight of TMP) = 4773.29 g/mol. Considering the error range of NMR integration, we used 4800 g/mol as the M_n value of the polymer **1**.

Synthesis of P(G_{56}-*co*-BAG_2). The Boc-protected P(G_{56}-*co*-$BBAG_2$) copolymer (polymer **1**) was dissolved in CH_2Cl_2 with trifluoroacetic acid (TFA) (1.0 mL) and stirred at room temperature for 1 h. The reaction mixture was concentrated under reduced pressure and the resulting deprotected polymer was dissolved in 1.0 mL of methanol; the homogeneous polymer solution was then precipitated in excess diethyl ether, and the precipitate was washed twice using diethyl ether. The resulting deprotected P(G_{56}-*co*-BAG_2) polymer was dried under vacuum at 90 °C for 1 day.

^{13}C NMR Kinetics. To generate the initiator, TMP (20 mg, 0.204 mmol), and potassium methoxide in methanol (25 wt %, 23 μL, 0.082 mmol) were reacted in a round-bottom flask under an argon atmosphere at 50 °C. Excess methanol was removed using a rotary evaporator, and the resulting product was dried in a vacuum oven at 90 °C for 3 h to yield a white salt of the initiator. The initiator was added to the comonomer mixture of G (0.151 g, 2.04 mmol) and BBAG (0.500 g, 2.04 mmol), which was placed in a 4.0 mL vial and stirred over an ice bath. The mixture was transferred to a conventional NMR tube under an argon atmosphere and then sealed with a septum over an ice bath. The kinetic measurements using ^{13}C NMR spectroscopy were recorded on a 600 MHz VNMRS system with a 5 mm PFG AutoXDB probe in neat solutions. A standard kinetic ^{13}C NMR experiment required 64 transients, which were obtained with a 13.7 μs 90° pulse, spectral width of 1894 Hz, and recycling delay of 10 s for each kinetic run; 43 experiments were performed over a period of 12 h with a flip angle of 45° and inverse gated decoupling.

Rhodamine B Conjugated Hyperbranched P(G_{113}-*co*-BAG_{21}) Polymer. Rhodamine B conjugated polymer was synthesized according to a method previously described in the literature.[36] *N*-Hydroxysuccinimide (2.3 mg, 0.02 mmol) and rhodamine B (9.6 mg, 0.02 mmol) were dissolved in 1.5 mL of DMF, and then *N*,*N*′-dicyclohexylcarbodiimide (6.2 mg, 0.03 mmol) and 4-dimethylaminopyridine (2.4 mg, 0.02 mmol) were added to the solution. The mixture was stirred at room temperature for 30 min, and then, 70 mg of P(G_{113}-*co*-BAG_{21}) (polymer **7**) in 1.5 mL of DMF was added to the solution. After stirring for 48 h at room temperature, the insoluble residue was filtered off and the solvent was removed by a rotary evaporator. The residues were dissolved in deionized water to dialyze against water for 7 days, followed by lyophilization to give the rhodamine B-conjugated polymer in a quantitative yield.

Cytotoxicity Assay. Murine macrophage cell line, RAW264.7, was purchased from the Korean Cell Line Bank (Seoul, Korea). Cytotoxicity assays were performed using the traditional MTT assay. Cells were seeded in 24-well plates at a density of 1×10^5 cells per well and incubated for 24 h in 5% CO_2 at 37 °C. The RAW264.7 cells were cultured with Dulbecco's Modified Eagle's Medium (DMEM, Hyclone) containing 10% fetal bovine serum (FBS) and 1% penicillin−streptomycin. After removing the culture medium, the wells were washed with phosphate-buffered saline (PBS). Each well was then treated with various concentrations of P(G-*co*-BAG) solutions (polymers **3**, **6**, and **7**) and incubated for an additional 18 h. For the MTT assays, each well was washed with PBS then filled with 60 μL of a thiazolyl blue tetrazolium bromide (MTT, Sigma-Aldrich) stock solution (5.0 mg/mL) and 940 μL of fresh media. After incubation for 3 h, 1.0 μL of DMSO was added to the polymer solution to solubilize the MTT-formazan product, after which the plates were gently agitated for 15 min at room temperature. After transferring 100 μL of each sample into the 96-well plates, the absorbance of the solution was recorded at a wavelength of 540 nm using 620 nm as the reference.

Cellular Uptake Imaging. Cellular uptake of the rhodamine B-conjugated polymers was tested by using HEK-293T cells. Cells were seeded on a coverslip in a 24-well tissue culture plate at a density of 1

DOI: 10.1021/acs.biomac.6b01136
Biomacromolecules 2016, 17, 3632−3639

Table 1. Characterization Data for the Synthesized P(G-*co*-BBAG) Copolymers

No.	polymer composition (target)	polymer composition[a] (NMR)	M_n (target)	%BBAG (target)	M_n[a] (NMR)	%BBAG[a] (NMR)	M_n[b] (GPC)	M_w/M_n[b] (GPC)
1	$P(G_{57}$-*co*-$BBAG_3)$	$P(G_{56}$-*co*-$BBAG_2)$	5093	5	4800	3.4	9000	1.3
2	$P(G_{52}$-*co*-$BBAG_6)$	$P(G_{61}$-*co*-$BBAG_8)$	5458	10	6600	11.6	10000	1.4
3	$P(G_{114}$-*co*-$BBAG_6)$	$P(G_{125}$-*co*-$BBAG_5)$	10051	5	10600	3.8	10000	1.4
4	$P(G_{100}$-*co*-$BBAG_{10})$	$P(G_{100}$-*co*-$BBAG_8)$	9995	10	9500	7.4	12200	1.6
5	$P(G_{228}$-*co*-$BBAG_{12})$	$P(G_{149}$-*co*-$BBAG_{11})$	19968	5	13900	6.9	8500	1.3
6	$P(G_{200}$-*co*-$BBAG_{22})$	$P(G_{170}$-*co*-$BBAG_{16})$	20347	10	16700	8.6	12600	1.5
7	$P(G_{100}$-*co*-$BBAG_{25})$	$P(G_{113}$-*co*-$BBAG_{21})$	13675	20	13700	15.7	6800	1.2

[a]Determined via ^{1}H NMR spectroscopy. [b]Measured using GPC-RI in DMF with a polystyrene standard.

$\times 10^5$ cells per well and incubated for 24 h. After the initial cell culture, the rhodamine B-conjugated polymer (polymer **7**) dissolved in water (0.50 mg/mL) was added to each well, and incubated at 37 °C for an additional 24 h. After washing with PBS (pH 7.4), a solution of 4′,6-diamidino-2-phenylindole (DAPI, Sigma-Aldrich; 20 mg/mL in MEM media) was incubated at 37 °C. After incubation for 30 min, the cells were fixed with 4% formaldehyde at room temperature. Confocal laser scanning microscopy (CLSM) images were taken using an Olympus FV1000 confocal microscope equipped with 405, 473, and 559 nm laser with fluorescence detection channels.

RESULTS AND DISCUSSION

The general synthetic routes toward the BBAG monomer and copolymers are outlined in Figure 1. In the first step, 4-amino-1-butanol was protected with di-*t*-butyl dicarbonate (Boc_2O) and triethylamine (TEA) in dichloromethane (DCM) to generate *t*-butyl *N*-(4-hydroxybutyl)carbamate. The intermediate was then coupled with epichlorohydrin to obtain a Boc-protected butanolamine glycidyl ether (BBAG) monomer, *t*-butyl 4-(oxiran-2-ylmethoxy)butylcarbamate. The successful synthesis of the BBAG monomer was confirmed through various charcterizations including ^{1}H and ^{13}C NMR, COSY, HMQC, and DEPT spectroscopy, and ESI-MS (see Figure 2 and Figures S1−S4 in the Supporting Information).

After successful synthesis of the BBAG monomer, we studied its anionic ring-opening multibranching polymerization using a potassium alkoxide initiator that was formed via the reaction of trimethylolpropane (TMP) and a potassium methoxide solution.[19] As demonstrated previously, we employed slow monomer addition of a mixture of G and BBAG monomer to the deprotonated TMP initiator and copolymerized at 90 °C for 17 h for a controlled synthesis of the polymers. The molecular weight of the copolymers was controlled by the monomer-to-initiator ratio and the comonomer feed ratio of BBAG to G monomers, which was varied from 5 to 20% to yield different degrees of BBAG incorporation within the copolymer.

The successful synthesis of P(G-*co*-BBAG) copolymers was characterized by ^{1}H NMR and GPC measurements (Figures 2, S6, and S7, and Table 1). As shown in Figure 2, the ^{1}H NMR spectra of the BBAG monomer and synthesized polymers indicated the corresponding characteristic proton peaks. Specifically, the M_n value was calculated by the ratio of the peak integrals between the methyl and methylene groups of the TMP initiator (peaks at 0.8 and 1.3 ppm, respectively) and polyether backbone (peaks at 3.3−3.8 ppm; see the Experimental Section for detailed calculations). In addition, the incorporation ratio of BBAG within the P(G-*co*-BBAG) copolymers was determined by integrating the unique distinguishable protons of the *t*-butyl group on BBAG (peak at 1.34 ppm) against the signal of the initiator and polyether backbone. Overall, we found reasonable agreement between the target molecular weight and composition and those obtained from the ^{1}H NMR results (Table 1).

The hyperbranched nature of the P(G-*co*-BBAG) copolymers was further confirmed by measuring the degree of branching (DB) via detailed analysis of the ^{13}C NMR spectra (Figures S8 and S9 and Table S1). The resulting DB indicated the ratio of the branched dendritic segment within the PG backbones, which were composed of both AB-type linear (BBAG block) and AB_2-type branched (G block) segments. The DBs of the selected polymers, polymer **5** and **7**, were determined to be about 0.63 and 0.56, which were in a similar ranges with those of other hyperbranched systems.[15,33,37]

The GPC results showed controlled molecular weight values with a monomodal distribution (Table 1 and Figure S10). The M_n of the copolymers was found to be 6800−12600 with a polydispersity index (M_w/M_n) value of 1.2−1.6 determined by GPC using polystyrene as a standard. It is of note that there is an observable discrepancy between the molecular weights determined by ^{1}H NMR and GPC; however, this could be attributed to the hyperbranched architecture and presence of multiple hydroxyl functional groups because these globular hyperbranched structures do not contribute to the overall hydrodynamic radius of the polymers. Additionally, the use of linear polystyrene as a molecular weight reference could lead to the deviation.

The Boc-protected copolymers were treated with trifluoroacetic acid (TFA) for 1 h to yield the desired P(G-*co*-BAG) copolymers. The elimination of the Boc moiety was clearly monitored in the ^{1}H NMR spectrum with the disappearance of the strong *t*-butyl group at 1.34 ppm (Figure 2c). Moreover, the ^{13}C NMR analysis supported the removal of Boc group as well (Figure S11). Besides these spectroscopic analyses, a simple ninhydrin assay confirmed the successful recovery of the primary amine groups. The synthesized P(G-*co*-BBAG) copolymers and deprotected P(G-*co*-BAG) copolymers were soluble in organic polar solvents such as methanol, DMSO, and DMF. The P(G-*co*-BBAG) copolymers were moderately soluble in water; however, P(G-*co*-BAG) copolymers became highly soluble in water after deprotection (Figure S7).

Analysis of polymers bearing primary amine groups with GPC is rather challenging due to the strong interaction between amine groups and GPC columns. However, acetylation of the amine groups allows the characterization of copolymers after the deprotection.[27] As a representative example, GPC analysis of polymer **7** after the treatment with excess acetic anhydride demonstrated a clear monomodal trace with a narrow polydispersity index of 1.15, further confirming the successful polymerization and subsequent functionality (Figure S12).

DOI: 10.1021/acs.biomac.6b01136
Biomacromolecules 2016, 17, 3632−3639

Along with the successful synthesis of the desired copolymers, we also attempted the homopolymerization of the novel BBAG monomer; however, the resulting BBAG homopolymer did not dissolve at all in many common solvents (i.e., chloroform, dichloromethane, THF, dioxane, ethyl acetate, methanol, ethanol, DME, DMSO, DMF, chlorobenzene, and trichlorobenzene) after recovering the precipitate, which limited the structural analysis of the homopolymers. The insoluble precipitate does not become soluble even after the treatment of TFA, suggesting possible cross-linking reaction during the homopolymerization of the BBAG monomer. A model reaction using *tert*-butyl 4-methoxybutylcarbamate, similar to the chemical structure of side chain of the butanolamine glycidyl ether, further suggested that there could be possible deprotection of Boc groups when both strong base and high temperature were employed together. Although the degree of deprotection was less than 5% under current polymerization condition, it increased with increasing equivalence of strong base under high temperature. Nonetheless, when copolymerized with the G monomer, the relative fraction of the BBAG to G was relatively small within the range of 5−20%, thus, possible side reaction occurring on the Boc group could be reduced significantly. This postulation is further supported by comparison of the NMR integration of the two internal peaks such as polyether backbone and Boc peaks with respect to the TMP initiator, suggesting no considerable deprotection of the Boc group during the copolymerization.

As we developed the novel BBAG monomer, it was essential to investigate its copolymerization behavior with other monomers. In order to investigate the kinetics of two monomers during copolymerization, in situ ^{13}C NMR kinetic measurements were performed on the basis of recent developments reported by Frey and co-workers (Figure 3).[38,39] Specifically, the copolymerization of G and BBAG monomers at an equimolar ratio was performed in a conventional NMR tube at 75 °C. During bulk polymerization, a quantitative ^{13}C NMR spectrum could be obtained within a few minutes due to the sufficient abundance of the ^{13}C isotope.

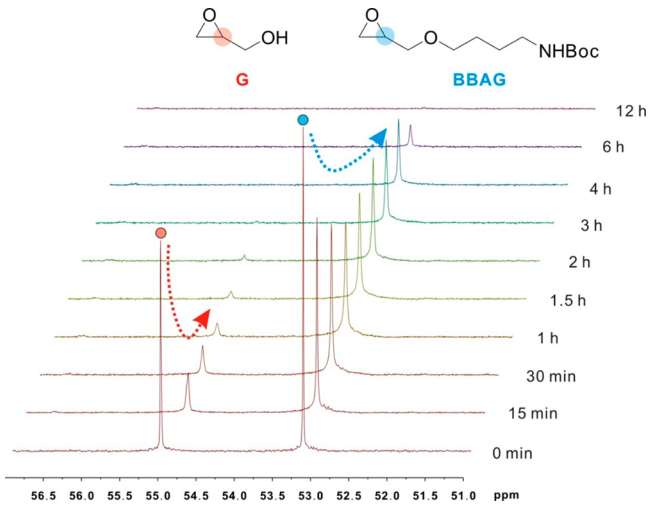

Figure 3. ^{13}C NMR spectra of the in situ copolymerization kinetics of G and BBAG monomers (initial monomer ratio of 1:1). Overlay of the spectra showing the signals for the methine carbons of the epoxide at 54.9 and 53.2 ppm, which correspond to the G and BBAG monomers, respectively, collected after the designated time period (DMSO-d_6, 150 MHz, 75 °C).

Figure 3 shows a series of ^{13}C NMR spectra collected during the copolymerization of G and BBAG monomers, which demonstrate the consumption of both monomers with the progress of polymerization. To evaluate the monomer consumption in a quantitative manner, the resonance peaks corresponding to the representative methine carbon for both epoxide monomers (at 54.9 and 53.2 ppm for G and BBAG, respectively) was compared during copolymerization. The disappearance of the G monomer was very rapid and it was difficult to evaluate the initial consumption, even after 15 min of the reaction at 75 °C. The reduced reactivity of BBAG can be attributed to the structure of the long alkyl spacer within BBAG, which could have hindered the ring-opening from other epoxide monomers, as has been similarly observed in other studies involving functional epoxide monomers.[17,19] In addition, the stability of ring-opening product of secondary alkoxide chain end from the BBAG monomer is considerably lower than that of primary alcolate resulting from the fast proton transfer reaction of the G monomer. Thus, more stable alkoxide chain end generated from the G monomer suppresses the backward reaction, which in turn increases the rate of G conversion.

The monomer conversion ratio of both G and BBAG monomers was plotted against the total conversion ratio during copolymerization (Figure 4). The monomer conversion in the

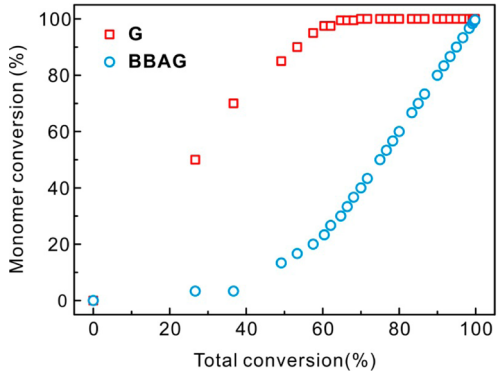

Figure 4. Monomer conversion percentage versus total conversion for copolymerization of G (red square) and BBAG (blue circle; initial monomer ratio of 1:1) determined from quantitative ^{13}C NMR kinetics at 75 °C.

first ^{13}C NMR spectra was set to 0% and the conversion ratio was calculated from the integration values of the methine group of each monomer against the signal from the Boc-protecting group, which remained constant during polymerization. As shown clearly in Figure 4, the molar ratio of the BBAG unit in the polymer chain was considerably lower than the monomer feed at the initial stage and increased rapidly upon consumption of the G monomer near the final stages of the reaction; for instance, at a total conversion of ∼50%, the conversions of G and BBAG were 78 and 19%, respectively. Thus, there is a gradient of monomer incorporation during copolymerization of P(G-*co*-BBAG). However, it should be noted that the kinetic experiments were conducted in a batch polymerization, which typically highlights the difference in the kinetics of the two different monomers during the copolymerization. On the other hand, in our actual copolymerization process in which the slow monomer addition method for a long period of time in a solution was employed could reduce this difference considerably, as reported similarly in literature.[40] Thus, we postulate

DOI: 10.1021/acs.biomac.6b01136
Biomacromolecules 2016, 17, 3632−3639

that the gradient nature of the copolymerization will be significantly reduced and the chain ends will be in a statistical mixture of alcohols (from G monomer) and amines (from BBAG monomer).

MALDI-ToF spectrometry was performed to confirm the incorporation of G and BAG monomers within the copolymer backbone and the successful deprotection of the Boc group as well (Figure 5). Moreover, it augments the GPC analysis due to

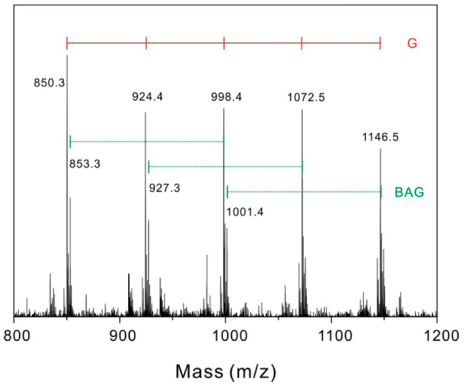

Figure 5. Expanded MALDI-ToF mass spectrum of the P(G_{125}-*co*-BAG_5) copolymer (polymer 3) from 800 to 1200 Da. The spacing of the signals corresponds to the mass of the respective monomers in the copolymer (G: 74.08 g/mol and BAG: 145.2 g/mol).

the inherent limitation in characterization of free amine groups within the P(G-*co*-BAG) copolymers. The presence of functional monomer segments in P(G-*co*-BAG) copolymers is revealed by peak analysis as shown in Figure 5. For example, the spacing of the signals corresponds to the mass of a linear combination of the respective monomers in the copolymer in varying degrees, which unambiguously demonstrates the successful copolymerization and deprotection of P(G-*co*-BAG) copolymers.

Upon successful demonstration of the deprotection to release the free amino groups within the polymers, we evaluated the charge density by zeta potential measurement. As expected, the synthesized P(G-*co*-BAG) copolymers displayed highly positive charges between 24.4 and 34.9 mV, which suggested potential applications as prospective DNA and siRNA carriers (Table 2). We observed that the higher amount of amine functional groups in P(G-*co*-BAG) generally led to a higher zeta potential. Moreover, the thermal properties and microstructure of the copolymers were investigated with differential scanning calorimetry (DSC), as summarized in Table 2. The glass transition temperature (T_g) for the P(G-*co*-BBAG) copolymers were ranged between −52.7 and −31.8 °C, which increased to between −30.9 and −5.6 °C upon deprotection to afford the P(G-*co*-BAG) copolymers. The T_g of the copolymers increased generally with increasing BAG contents and decreasing molecular weights. The additional intermolecular interactions present in the BAG group affect the T_g value of hyperbranched copolymers, as compared with pure PGs synthesized in our previous study (i.e., PG_{75}, − 27.2 °C, and PG_{150}, − 32.2 °C). In addition, the appearance of a single T_g for copolymers in the DSC curves suggests successful copolymerization without phase separation between the comonomers.

Encouraged by the successful synthesis of P(G-*co*-BAG) copolymers with active amine groups, we evaluated their cytotoxicity to investigate their potential in biomedical settings. Three representative polymers with varying degree of amine contents (from 3.8%, 8.6% to 15.7% for polymers **3**, **6**, and **7**, respectively) were treated with the murine macrophage cell line, RAW264.7 as a model normal cell. The cytotoxicity of each polymer was examined using an MTT assay based on the mitochondrial dehydrogenase activity. As shown in Figure 6a, the cell viability of each cell line treated with various concentrations of the polymer solution was greater than 95%, even up to a concentration of 500 μg mL^{-1}, which is usually beyond the common concentration ranges tested. Although many polyamines are reported to display significant cytotoxicity due to the free amine groups associated with tight cell binding,[41,42] our P(G-*co*-BAG) copolymers exhibited considerably low cell toxicity; this is attributed to the protected amine groups sheathed by the hyperbranched PG shell, yielding optimum cell viability.

The facile functionalization of amine groups sheathed within the framework of hyperbranched PG could provide a useful platform for further modification with other organic or biological molecules.[43,44] Toward this end, the available amine groups within the P(G-*co*-BAG) copolymers were further utilized to conjugate with a model dye, rhodamine, via a carbodiimide intermediate to yield the rhodamine B-conjugated P(G-*co*-BAG) copolymers. After preparation, their cellular uptake was further evaluated by confocal laser scanning microscopy (CLSM). Figure 6b clearly shows that the red fluorescence of the rhodamine B-conjugated copolymer stems from the localization of P(G_{113}-*co*-BAG_{21}) primarily within the perinuclear cytoplasm region, whereas the polymer is not located within the cell nucleus. This result indicates that the cellular uptake of hyperbranched P(G-*co*-BAG) is based on endocytosis. Taken together these cellular assay results with a high potential of conjugation chemistry, the hyperbranched P(G-*co*-BAG) copolymer with the novel amine moieties will offer a compelling platform for next-generation biological and biomedical materials.

Table 2. Characterization Data for the Synthesized P(G-*co*-BAG) Copolymers

		polymer composition (NMR)		T_g/°C (DSC)		
No.	polymer composition (target)	before	after deprotection	before	after	zeta potential (mV)
1	P(G_{57}-*co*-$BBAG_3$)	P(G_{56}-*co*-$BBAG_2$)	P(G_{56}-*co*-BAG_2)	−31.8	−18.7	24.4 ± 0.7
2	P(G_{52}-*co*-$BBAG_6$)	P(G_{61}-*co*-$BBAG_8$)	P(G_{61}-*co*-BAG_8)	−39.5	−25.1	27.7 ± 1.5
3	P(G_{114}-*co*-$BBAG_6$)	P(G_{125}-*co*-$BBAG_5$)	P(G_{125}-*co*-BAG_5)	−52.7	−30.9	24.0 ± 2.2
4	P(G_{100}-*co*-$BBAG_{10}$)	P(G_{100}-*co*-$BBAG_8$)	P(G_{100}-*co*-BAG_8)	−39.2	−26.0	25.9 ± 5.3
5	P(G_{228}-*co*-$BBAG_{12}$)	P(G_{149}-*co*-$BBAG_{11}$)	P(G_{149}-*co*-BAG_{11})	−34.5	−7.1	34.9 ± 1.1
6	P(G_{200}-*co*-$BBAG_{22}$)	P(G_{170}-*co*-$BBAG_{16}$)	P(G_{170}-*co*-BAG_{16})	−33.2	−22.9	25.5 ± 2.0
7	P(G_{100}-*co*-$BBAG_{25}$)	P(G_{113}-*co*-$BBAG_{21}$)	P(G_{113}-*co*-BAG_{21})	−33.2	−5.6	31.3 ± 3.1

DOI: 10.1021/acs.biomac.6b01136
Biomacromolecules 2016, 17, 3632−3639

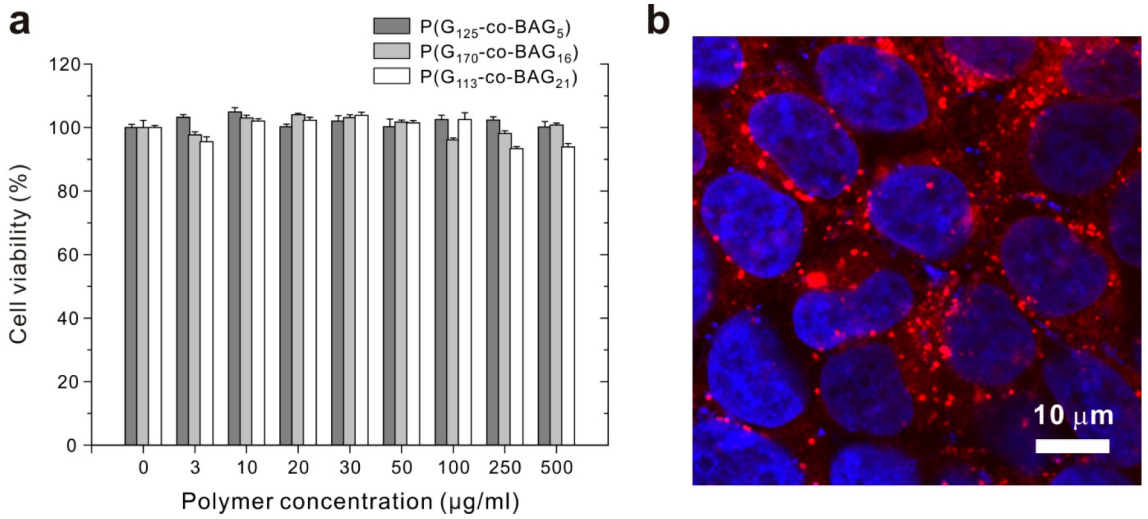

Figure 6. (a) In vitro cell viability assay of copolymers. P(G_{125}-*co*-BAG_5) (polymer **3**; dark gray), P(G_{170}-*co*-BAG_{16}) (polymer **6**; light gray), and P(G_{113}-*co*-BAG_{21}) (polymer **7**; white) polymers determined by MTT assays using RAW264.7 cell lines. (b) CLSM image of HEK293T cells incubated with rhodamine B-conjugated P(G_{113}-*co*-BAG_{21}) (polymer **7**). DAPI was used to stain the cell nucleus.

CONCLUSION

In summary, we present a one-pot synthesis of a series of hyperbranched PGs possessing amino functionality. A novel amino glycidyl ether as a monomer, Boc-protected butanolamine glycidyl ether monomer (BBAG), was designed and polymerized with glycidol (G) through anionic ring-opening multibranching polymerization to yield a well-defined P(G-*co*-BBAG) with an adjustable comonomer ratio, which was subsequently deprotected with TFA to yield the desired P(G-*co*-BAG) copolymers. The polymerization was successfully characterized by ^{1}H NMR and GPC, and the copolymerization kinetics between the two monomers was further revealed by an in situ ^{13}C NMR study. The high zeta-potential and in vitro biocompatibility assay results of P(G-*co*-BAG), together with its efficiency in conjugating functional molecules, clearly demonstrate its significant potential in bioconjugation chemistry, which takes advantage of the free amine groups sheathed in hyperbranched PGs. We anticipate that the new class of amine functional monomer and polymers developed in this study will contribute to the advancement and understanding of PG-based polymers and will be a promising candidate for emerging materials and biomedical applications.

ASSOCIATED CONTENT

Supporting Information

The Supporting Information is available free of charge on the ACS Publications website at DOI: 10.1021/acs.biomac.6b01136.

Additional ^{13}C NMR, COSY, HMQC, and DEPT spectroscopy data of the monomers and ^{1}H and ^{13}C NMR of representative copolymers, and detailed calculation of DB and GPC traces of copolymers (PDF).

AUTHOR INFORMATION

Corresponding Author

*E-mail: bskim19@unist.ac.kr.

Author Contributions

†These authors contributed equally to this work (S.S. and J.L.).

Notes

The authors declare no competing financial interest.

ACKNOWLEDGMENTS

This work was supported by the 2016 UNIST research fund (1.160001.01) and by the National Research Foundation of Korea (NRF; 2010-0028684, 2014R1A2A1A11054491). We acknowledge Prof. Hyun-Woo Rhee at UNIST for support in the confocal fluorescence microscopy.

REFERENCES

(1) Albertazzi, L.; Mickler, F. M.; Pavan, G. M.; Salomone, F.; Bardi, G.; Panniello, M.; Amir, E.; Kang, T.; Killops, K. L.; Bräuchle, C.; Amir, R. J.; Hawker, C. J. *Biomacromolecules* **2012**, *13*, 4089−4097.
(2) Dey, P.; Adamovski, M.; Friebe, S.; Badalyan, A.; Mutihac, R.-C.; Paulus, F.; Leimkühler, S.; Wollenberger, U.; Haag, R. *ACS Appl. Mater. Interfaces* **2014**, *6*, 8937−8941.
(3) Knop, K.; Hoogenboom, R.; Fischer, D.; Schubert, U. S. *Angew. Chem., Int. Ed.* **2010**, *49*, 6288−6308.
(4) Larson, N.; Ghandehari, H. *Chem. Mater.* **2012**, *24*, 840−853.
(5) Senevirathne, S. A.; Washington, K. E.; Biewer, M. C.; Stefan, M. C. *J. Mater. Chem. B* **2016**, *4*, 360−370.
(6) Pelegri-O'Day, E. M.; Lin, E.-W.; Maynard, H. D. *J. Am. Chem. Soc.* **2014**, *136*, 14323−14332.
(7) Thomas, A.; Müller, S. S.; Frey, H. *Biomacromolecules* **2014**, *15*, 1935−1954.
(8) Du, W.; Li, Y.; Nyström, A. M.; Cheng, C.; Wooley, K. L. *J. Polym. Sci., Part A: Polym. Chem.* **2010**, *48*, 3487−3496.
(9) Saville, P. M.; Reynolds, P. A.; White, J. W.; Hawker, C. J.; Frechet, J. M. J.; Wooley, K. L.; Penfold, J.; Webster, J. R. P. *J. Phys. Chem.* **1995**, *99*, 8283−8289.
(10) Herzberger, J.; Niederer, K.; Pohlit, H.; Seiwert, J.; Worm, M.; Wurm, F. R.; Frey, H. *Chem. Rev.* **2016**, *116*, 2170−2243.
(11) Kainthan, R. K.; Muliawan, E. B.; Hatzikiriakos, S. G.; Brooks, D. E. *Macromolecules* **2006**, *39*, 7708−7717.
(12) Sisson, A. L.; Papp, I.; Landfester, K.; Haag, R. *Macromolecules* **2009**, *42*, 556−559.
(13) Wilms, D.; Stiriba, S.-E.; Frey, H. *Acc. Chem. Res.* **2010**, *43*, 129−141.
(14) Zheng, Y.; Li, S.; Weng, Z.; Gao, C. *Chem. Soc. Rev.* **2015**, *44*, 4091−4130.
(15) Schömer, M.; Seiwert, J.; Frey, H. *ACS Macro Lett.* **2012**, *1*, 888−891.

DOI: 10.1021/acs.biomac.6b01136
Biomacromolecules 2016, 17, 3632−3639

(16) Christ, E.-M.; Hobernik, D.; Bros, M.; Wagner, M.; Frey, H. *Biomacromolecules* **2015**, *16*, 3297−3307.
(17) Niederer, K.; Schüll, C.; Leibig, D.; Johann, T.; Frey, H. *Macromolecules* **2016**, *49*, 1655−1665.
(18) Thomas, A.; Bauer, H.; Schilmann, A.-M.; Fischer, K.; Tremel, W.; Frey, H. *Macromolecules* **2014**, *47*, 4557−4566.
(19) Son, S.; Shin, E.; Kim, B.-S. *Macromolecules* **2015**, *48*, 600−609.
(20) Son, S.; Park, H.; Shin, E.; Shibasaki, Y.; Kim, B.-S. *J. Polym. Sci., Part A: Polym. Chem.* **2016**, *54*, 1752−1761.
(21) Meyer, J.; Keul, H.; Möller, M. *Macromolecules* **2011**, *44*, 4082−4091.
(22) Wurm, F.; Dingels, C.; Frey, H.; Klok, H.-A. *Biomacromolecules* **2012**, *13*, 1161−1171.
(23) Moore, E.; Delalat, B.; Vasani, R.; Thissen, H.; Voelcker, N. H. *Biomacromolecules* **2014**, *15*, 2735−2743.
(24) Pant, K.; Gröger, D.; Bergmann, R.; Pietzsch, J.; Steinbach, J.; Graham, B.; Spiccia, L.; Berthon, F.; Czarny, B.; Devel, L.; Dive, V.; Stephan, H.; Haag, R. *Bioconjugate Chem.* **2015**, *26*, 906−918.
(25) Su, Z.; Jiang, X. *Polymer* **2016**, *93*, 221−239.
(26) Koyama, Y.; Umehara, M.; Mizuno, A.; Itaba, M.; Yasukouchi, T.; Natsume, K.; Suginaka, A.; Watanabe, K. *Bioconjugate Chem.* **1996**, *7*, 298−301.
(27) Obermeier, B.; Wurm, F.; Frey, H. *Macromolecules* **2010**, *43*, 2244−2251.
(28) Reuss, V. S.; Obermeier, B.; Dingels, C.; Frey, H. *Macromolecules* **2012**, *45*, 4581−4589.
(29) Herzberger, J.; Frey, H. *Macromolecules* **2015**, *48*, 8144−8153.
(30) Isono, T.; Asai, S.; Satoh, Y.; Takaoka, T.; Tajima, K.; Kakuchi, T.; Satoh, T. *Macromolecules* **2015**, *48*, 3217−3229.
(31) Lee, A.; Lundberg, P.; Klinger, D.; Lee, B. F.; Hawker, C. J.; Lynd, N. A. *Polym. Chem.* **2013**, *4*, 5735.
(32) Son, S.; Shin, E.; Kim, B.-S. *Biomacromolecules* **2014**, *15*, 628−634.
(33) Oikawa, Y.; Lee, S.; Kim, D. H.; Kang, D. H.; Kim, B.-S.; Saito, K.; Sasaki, S.; Oishi, Y.; Shibasaki, Y. *Biomacromolecules* **2013**, *14*, 2171−2178.
(34) Lee, S.; Saito, K.; Lee, H.-R.; Lee, M. J.; Shibasaki, Y.; Oishi, Y.; Kim, B.-S. *Biomacromolecules* **2012**, *13*, 1190−1196.
(35) Nguyen, C.; Ruda, G. F.; Schipani, A.; Kasinathan, G.; Leal, I.; Musso-Buendia, A.; Kaiser, M.; Brun, R.; Ruiz-Pérez, L. M.; Sahlberg, B.-L.; Johansson, N. G.; González-Pacanowska, D.; Gilbert, I. H. *J. Med. Chem.* **2006**, *49* (14), 4183−4195.
(36) Pang, Y.; Zhu, Q.; Liu, J.; Wu, J.; Wang, R.; Chen, S.; Zhu, X.; Yan, D.; Huang, W.; Zhu, B. *Biomacromolecules* **2010**, *11*, 575−582.
(37) Sunder, A.; Hanselmann, R.; Frey, H.; Mülhaupt, R. *Macromolecules* **1999**, *32*, 4240−4246.
(38) Wolf, F. K.; Frey, H. *Macromolecules* **2009**, *42*, 9443−9456.
(39) Alkan, A.; Natalello, A.; Wagner, M.; Frey, H.; Wurm, F. R. *Macromolecules* **2014**, *47*, 2242−2249.
(40) Seiwert, J.; Leibig, D.; Kemmer-Jonas, U.; Bauer, M.; Perevyazko, I.; Preis, J.; Frey, H. *Macromolecules* **2016**, *49*, 38−47.
(41) Deng, Y.; Saucier-Sawyer, J. K.; Hoimes, C. J.; Zhang, J.; Seo, Y.-E.; Andrejecsk, J. W.; Saltzman, W. M. *Biomaterials* **2014**, *35*, 6595−6602.
(42) Mehrabadi, F. S.; Hirsch, O.; Zeisig, R.; Posocco, P.; Laurini, E.; Pricl, S.; Haag, R.; Kemmner, W.; Calderón, M. *RSC Adv.* **2015**, *5*, 78760−78770.
(43) Gröger, D.; Paulus, F.; Licha, K.; Welker, P.; Weinhart, M.; Holzhausen, C.; Mundhenk, L.; Gruber, A. D.; Abram, U.; Haag, R. *Bioconjugate Chem.* **2013**, *24*, 1507−1514.
(44) Zeng, H.; Schlesener, C.; Cromwell, O.; Hellmund, M.; Haag, R.; Guan, Z. *Biomacromolecules* **2015**, *16*, 3869−3877.

DOI: 10.1021/acs.biomac.6b01136
Biomacromolecules 2016, 17, 3632−3639